

HENRY

Hydraulic Engineering Repository

Ein Service der Bundesanstalt für Wasserbau

Conference Paper, Published Version

Mohammadnezhad, B. A.; Mohammadian, M.; Mohammadian, V. Numerical modeling of sedimentation in the Sefid-Rood Reservoir, Iran

Verfügbar unter/Available at: <https://hdl.handle.net/20.500.11970/99761>

Vorgeschlagene Zitierweise/Suggested citation:

Mohammadnezhad, B. A.; Mohammadian, M.; Mohammadian, V. (2010): Numerical modeling of sedimentation in the Sefid-Rood Reservoir, Iran. In: Dittrich, Andreas; Koll, Katinka; Aberle, Jochen; Geisenhainer, Peter (Hg.): River Flow 2010. Karlsruhe: Bundesanstalt für Wasserbau. S. 1131-1138.

Standardnutzungsbedingungen/Terms of Use:

Die Dokumente in HENRY stehen unter der Creative Commons Lizenz CC BY 4.0, sofern keine abweichenden Nutzungsbedingungen getroffen wurden. Damit ist sowohl die kommerzielle Nutzung als auch das Teilen, die Weiterbearbeitung und Speicherung erlaubt. Das Verwenden und das Bearbeiten stehen unter der Bedingung der Namensnennung. Im Einzelfall kann eine restriktivere Lizenz gelten; dann gelten abweichend von den obigen Nutzungsbedingungen die in der dort genannten Lizenz gewährten Nutzungsrechte.

Documents in HENRY are made available under the Creative Commons License CC BY 4.0, if no other license is applicable. Under CC BY 4.0 commercial use and sharing, remixing, transforming, and building upon the material of the work is permitted. In some cases a different, more restrictive license may apply; if applicable the terms of the restrictive license will be binding.



Numerical Modeling of Sedimentation in the Sefid-Rood Reservoir, Iran

Bayram Ali Mohammadnezhad

Department of Water Engineering, University of Umiah, Iran

Majid Mohammadian

Department of Civil Engineering, University of Ottawa, Canada

Vahid Mohammadian

Department of Civil Engineering, Chabahar Maritime University, Iran

ABSTRACT: Sedimentation is one of the major problems in dam reservoirs. Accumulation of sediment in reservoirs reduces the water capacity of the reservoirs and also leads to erosion problems in the rivers downstream since the sediment load in the river is no longer in a condition of equilibrium. Opening of sluice gates is a common method for the evacuation of sediment. However, optimal opening and closing of gates requires accurate information about the density current in the reservoir. In this paper, the evolution of density current in the reservoir of the Sefid-Rood Dam in Iran is simulated using the Mike 3 model with an unstructured grid, and the numerical results are compared with field measurements.

Keywords: Density current, Sedimentation, Sediment evacuation, Sluice gates, Numerical modeling

1 INTRODUCTION

The Sefid-Rood Dam is situated about 200 km northwest of Iran at the intersection of Ghezel-Ozan and Shah-Rood Rivers. The Ghezel-Ozan River, which is the main branch of Sefid-Rood, originates from mountains in Kurdistan and Azerbaijan, with a maximum discharge of 2000 m³/s and a minimum discharge of 50 L/s and is 500 km long upstream of the dam. The Shah-Rood River originates from the Alamot and Taleghan Mountains with a discharge between 4.2-800 m³/s, and is 180 km long upstream of the dam. The maximum total inflow discharge occurs in April. The Sefid-Rood Dam, constructed in 1960, is a concrete dam with a capacity of 1.8 x 10⁹ m³. It is 106m high from its foundation and the dam crown is 86m higher than the riverbed. The length of the dam at the crown is 425m and its width is 5m at the crown and 106m at the foundation. The main purposes of the dam are retaining water, controlling floods, and power generation. The maximum surface area of the reservoir is 56 km² and the surface of the watershed basin is 56,200 km². The dam has three sluice gates at the bottom with a total capacity of 550 m³/s, two mid-depth outlets with a total capacity of 2,000 m³/s, and two spillways with a total capacity of 3,200 m³/s. Downstream of the Sefid Rood Dam, there are two smaller dams, the Tarik and Sangar Dams. The

present study deals with sedimentation in reservoirs and the case study of the Sefid-Rood Dam.



Figure 1. The Sefid-Rood Dam at the intersection of two rivers.



Figure 2. The downstream river of the Sefid-Rood dam.

The circulation of water in dam reservoirs in general is a three-dimensional current which depends on various parameters, such as bathymetry,

climate, and hydrologic conditions. A large volume of sediment enters into the reservoir during flood conditions over a short period of time. Such flows have a high density due to their carrying a large volume of sediment. Therefore, because of the difference between the density of the flood and the reservoir waters, the floodwater flows under the reservoir clear-water as a stratified flow. This under-flow, which is called density current, carries a large volume of sediment towards the dam. Therefore, in order to perform optimal opening and closing of the gates, it is essential to predict and simulate the density current, which is the subject of this paper, for the Sefid-Rood Dam.

2 DENSITY CURRENT

Density currents are caused by gravity effects and are controlled by several factors, such as the geometry of the reservoir (slope, depth, and width), stratification, the difference between the density of the inflow and reservoir water, and the flow regime in the river. Such currents may occur in the form of jets or plumes, flowing upward or downward.

The difference in density may be caused by temperature, sediment, dissolved salt, etc. Temperature difference leads to convective flows; e.g., in cooling systems of power plants, or in reservoirs due to seasonal weather changes. For example, cold winter weather leads to an overturn in reservoirs. Suspended sediments also increase the density which leads to underflows (or mid-depth currents) and has a great impact on sedimentation processes in reservoirs. Density currents can also carry considerable nutrients or chemical material and therefore are very important in environmental studies. Field measurements have revealed that such flows can reach a speed of 2 m/s and extend over 100 km.

Density currents are more apparent in deep reservoirs with a steep bed slope when the sediment concentration of the inflow is high. The favorable conditions for turbidity current development in reservoirs are:

- Significant density difference (high concentration),
- deep reservoir,
- Low flow velocity,
- Steep slope of the channel entrance,

A straight alignment of the ground channel at the bottom through which the current flows as a compact jet under the clear water (Scheuerlein 1987). Density current may be characterized by the following criterion:

$$\frac{U^2}{\left(\frac{\rho_s - \rho}{\rho_s}\right)gh} < Const \quad (1)$$

where U is the mean flow velocity, h = the flow depth, ρ_s = the density of turbidity current, ρ is the density of the reservoir fluid above turbidity current, g is the gravitational acceleration and $const = 0.6$ (after Zhang Hao et al. 1976) or 1.0-2.0 (after Buttlig & Shaw 1973 [1]), or by criterion proposed by Rooseboom (1975):

$$\frac{\partial u}{\partial x} + \frac{\partial v}{\partial y} + \frac{\partial w}{\partial z} = S \quad (2)$$

$$\begin{aligned} \frac{\partial u}{\partial t} + \frac{\partial u^2}{\partial x} + \frac{\partial uv}{\partial y} + \frac{\partial uw}{\partial z} = f_v - g \frac{\partial \eta}{\partial x} - \frac{1}{\rho_0} \frac{\partial P_a}{\partial x} - \frac{g}{\rho_0} \int_z^\eta \frac{\partial \rho}{\partial x} dz \\ + \frac{\partial}{\partial x} \left(2A \frac{\partial u}{\partial x} \right) + \frac{\partial}{\partial y} \left(A \left(\frac{\partial u}{\partial y} + \frac{\partial v}{\partial x} \right) \right) + \frac{\partial}{\partial z} \left(v_t \frac{\partial u}{\partial z} \right) + u_s S \end{aligned} \quad (3)$$

$$\begin{aligned} \frac{\partial v}{\partial t} + \frac{\partial uv}{\partial x} + \frac{\partial v^2}{\partial y} + \frac{\partial vw}{\partial z} = f_u - g \frac{\partial \eta}{\partial y} - \frac{1}{\rho_0} \frac{\partial P_a}{\partial y} - \frac{g}{\rho_0} \int_z^\eta \frac{\partial \rho}{\partial y} dz \\ + \frac{\partial}{\partial x} \left(A \left(\frac{\partial u}{\partial y} + \frac{\partial v}{\partial x} \right) \right) + \frac{\partial}{\partial y} \left(2A \frac{\partial v}{\partial y} \right) + \frac{\partial}{\partial z} \left(v_t \frac{\partial v}{\partial z} \right) + v_s S \end{aligned} \quad (4)$$

$$\frac{S_0 C^2 D^2}{Q^2} > 10000 \quad (5)$$

where S_0 is the average bed slope, C = the Chezy roughness coefficient, D = the average reservoir depth and Q = the discharge.

When the above condition is met, the flow may be characterized as a density current.

The density current moves towards the dam due to the gravity effect. Once the flow reaches the dam, a lake of mud is created and the sediment is gradually deposited.

3 THE MIKE 3 MODEL

Mike 3 is a three-dimensional numerical model developed by the Danish Hydraulic Institute for simulation of free-surface flows, cohesive/non-cohesive sediment transport, and water quality, using structured or unstructured grids. The employed equations are given by where x , y , and z are Cartesian coordinates, u , v , and w are the corresponding velocity components, η is the water surface elevation, $f = 2\Omega \sin \phi$ is the Coriolis parameter, p is the pressure, P_a is the atmospheric pressure, ρ is the density of water, ρ_0 is a reference density, v_t and A are horizontal and vertical eddy viscosity respectively, and S is the source or sink of water (with velocities u_s and v_s). We refer the reader to Mike 3 manual for the sediment transport equations and further details.

The model uses a finite volume method for numerical integration of equations. An unstructured grid is used in this study.

4 BOUNDARY CONDITIONS

Boundary conditions were specified at the inflow boundaries (Sefid-Rood and Shahrood Rivers) and outflow gates. The daily discharge hydrograph for 36 days (April 11, 2007 to May 16, 2007) was used because a flood condition occurred in that period of time and field measurements of the density current were also conducted.

The sediment concentrations at the inflow and at the downstream river were determined by sampling at 8:00 AM. The sediment samples were divided into three parts: clay, silt, and sand. The individual concentrations of sediment at each gate were estimated from the computational points upstream of the outlets, which is an approach commonly used for outflow boundary conditions. Daily measurements of precipitation and evaporation were available and were used as mass source/sink terms.

5 OTHER INPUT DATA

A time step size of 60s was chosen due to stability considerations. The maximum resulting CFL number for the hydrodynamic model is 0.26, and for the advection-diffusion model 0.48, which are both in the stability range of the model.

The effects of temperature and salinity on the density were negligible and were ignored. Wetting and drying of computational cells were allowed in the simulations. Turbulence was modeled using a combined $k-\epsilon$ and Smagourinski model. The Coriolis and wind effects were small in this case and were ignored. The bed roughness height was assumed to be 0.05 m based on bed material samples. The initial water surface elevation based on measured data was 264.93m above sea level. The initial sediment concentration of water in the reservoir was assumed to be zero (i.e. clear water). Ten vertical levels employed in the model were uniformly distributed as shown in Figure 3.

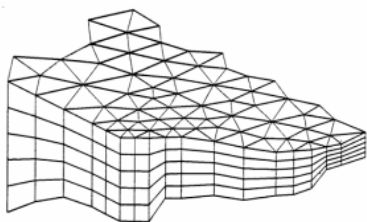


Figure 3. A schematic view of the numerical grid

The computational grid developed for this system is shown in Figure 3. The grid size is smaller

close to the main stream and also vertical layers are closer to one another at the bottom for a better representation of the density current.

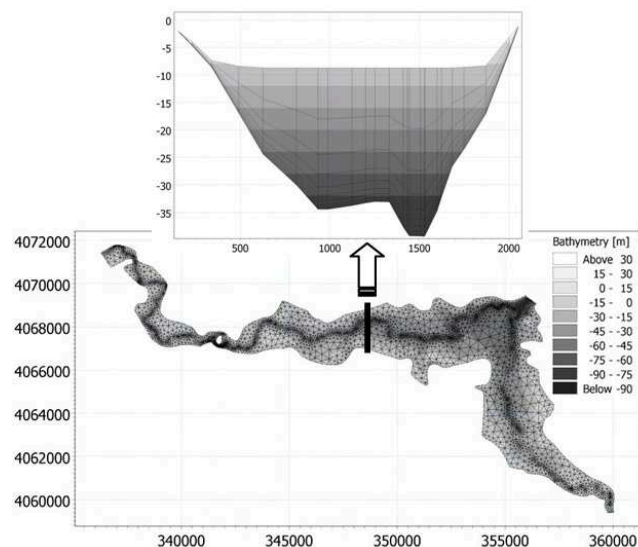


Figure 4. Horizontal grid and a typical vertical section

6 SIMULATIONS

Both Mike 21 and Mike 3 models were employed in this study and compared with measured field data over the simulation period. The field measurements were performed by the Water Research Institute. The inflow hydrographs for the two rivers, the outflow hydrographs corresponding to each outlet, and suspended sediment concentration hydrographs for two rivers at the entrance of reservoir are shown in Figures 5-a, 5-b, and 5-c respectively.

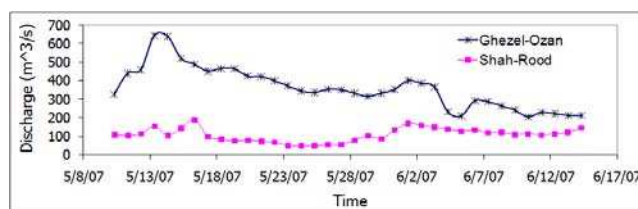


Figure 5-a. The inflow hydrographs of the two rivers

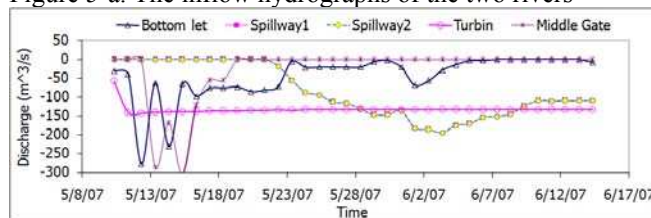


Figure 5-b. The outflow hydrographs of the outlets

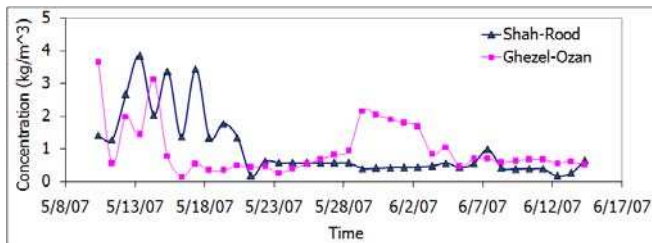


Figure 5-c. The suspended sediment concentration of the two rivers Inflows

Daily measurements of the Sefid-Rood and Shahrood Rivers at two stations just upstream of the reservoir were performed. The concentration of sediment close to the bed was measured. If the concentration was high, the flow was considered to be dense, and consequently sampling and sediment measurements were performed at all stations shown in Figure 6. Those data were employed in calibration of the model.

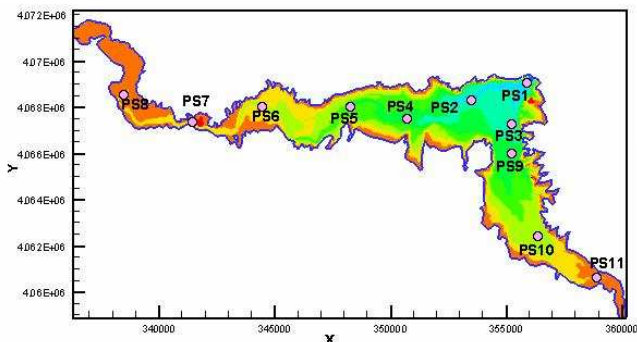


Figure 6. Location of sampling and concentration measurements on the dam reservoir

Numerical results of the Mike 21 model were largely different than the Mike 3, as expected due to existence of a non-uniform velocity profile throughout the water column. Therefore, we only present the results of the 3D model. Figure 8 shows the concentration of sediment on April 11, 2007 (2:00 PM) at a vertical section of the Ghezel-Ozan branch. The front of the density current can be clearly observed in this figure. A vertical section of the concentration of sediment at the Shahrood branch is also shown in Figure 8, which shows that the model can qualitatively represent the general form of density currents.

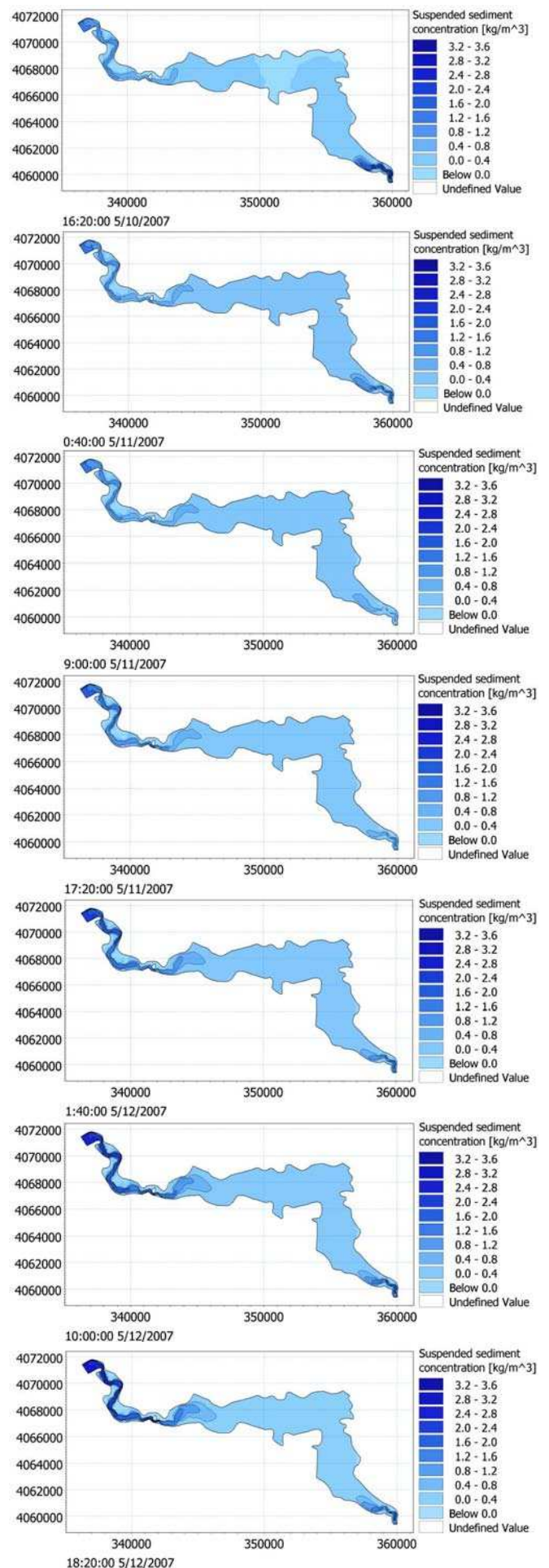


Figure 7. The concentration plots with time after initiation of the flood

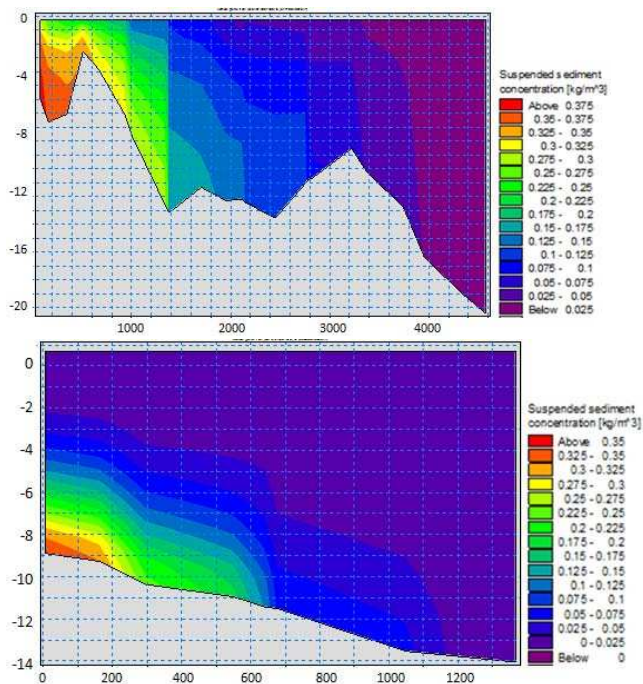


Figure 8. Vertical section of the concentration of sediment on April, 11, 2007 at 2:00 PM at the Ghezel-Ozan branch (up) and Shahrood branch (down).

Figure 9 shows a comparison of simulated and measured flow velocities at the section specified in Figure A-2. As can be seen, a reasonable agreement is observed between measurements and simulation.

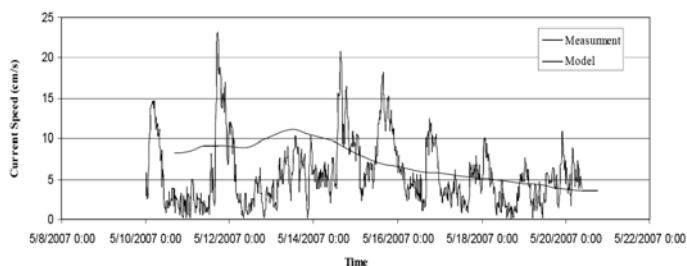


Figure 9. A comparison of the simulated current speed with field measurements at the section specified in Figure A-2

Once the accuracy of the model is confirmed, it can be used to gain an insight into the flow field in the reservoir. We begin with a general overview of the flow field, and then we will analyze the velocity profile in several sections of the two rivers and the reservoir. Figure 10 shows the contours of the u and v components of the velocity vector on day 11 of the simulation. As can be seen, the flow velocity is high on the Gazal-Ozan branch (around 1.5 m/s). The flow undergoes a meandering form and the velocity is reduced when the flow enters the reservoir. However, in the Shahrood branch, the length of the flow channel is less than the Gazal-Ozan branch and its flow reaches the dam sooner. The vertical velocity (w) is small everywhere and does not exceed 0.02 m/s.

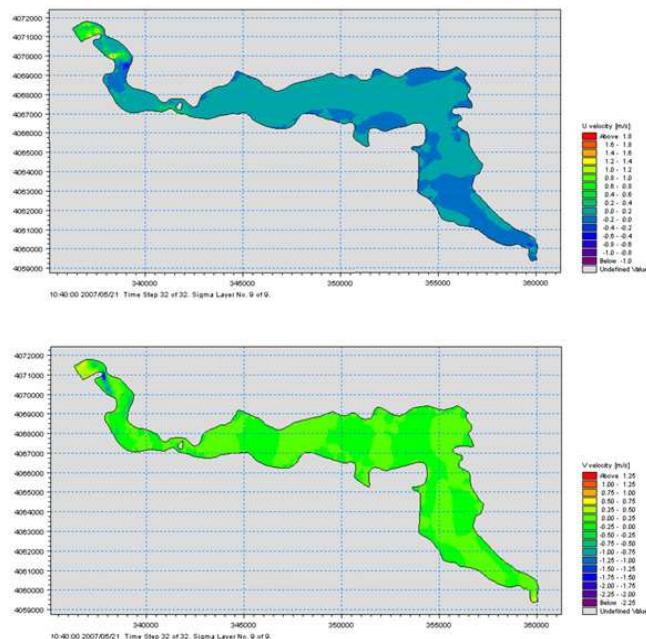


Figure 10. Contours of the u (up) and v (down) components of the velocity vector

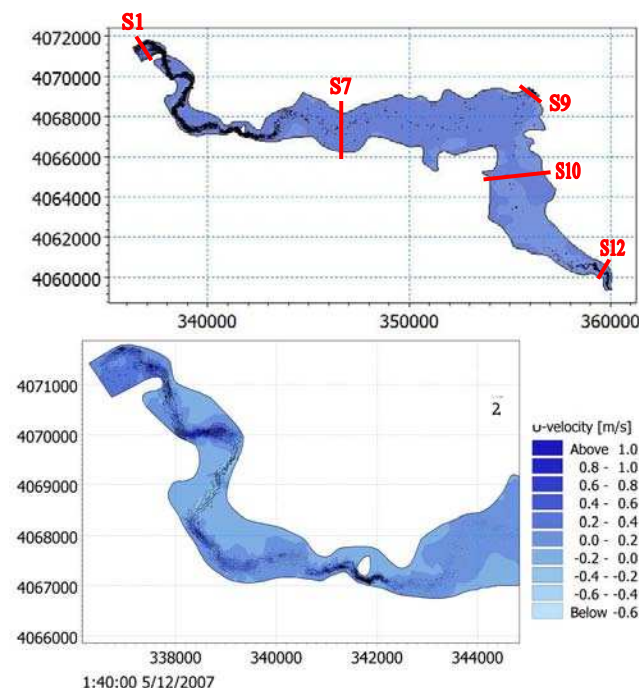


Figure 11. Velocity vectors and contours of the u component of the velocity vector.

Figure 11 shows the velocity vectors on day 11. The meandering form of the Gazal Ozan River is clear in this figure and shows that the flow maintains its high velocity over a long distance. This behavior significantly influences the travel time of the density current towards the dam. The Gazal-Ozan branch has a greater impact on the flow field than the Shahrood River; however, the density current of the Shahrood River reaches the dam faster and therefore determines the opening time of the gates. Several cross-sections on the two rivers and the reservoir are considered here (Figure 11) to gain an insight into the flow field and the evolution of the density current. Figure 12

shows the total velocity contour and its three components at section 1 on day 11. Two main channels with roughly equal depths are observed in this section. Maximum velocities of about 1.9 m/s occur at the sides, which is counter-intuitive. The w component of the velocity field is very small. The flow is more directed to the right side (when facing downstream) of the island and the maximum velocity occurs at the right side. Figure 13 shows the velocity contours at sections 7 and 9 on day 11. Section 7 is inside the reservoir, and water depth exceeds 40m in this section. The flow velocity is considerably decreased in this section and the main channel flow is diminished. Maximum velocity is less than 0.03 m/s close to the left side. Section 9 is just behind the dam, in which the maximum water depth is about 70m. The maximum velocity is observed around the center, which is due to the sluice gates. Figure 14 shows the velocity contours at sections 10 and 12 on the Shahrood River section. The maximum water velocity in section 10 occurs in the center, and another local maximum is observed on the right side. The maximum velocity in section 12 is about 0.44 m/s and is located around the center. Therefore, the flow in the Shahrood branch is roughly symmetric, unlike the Ghezal-Ozan branch. This leads to more mixing of the density current before reaching the dam than the Ghezal-Ozan flow, and therefore opening the gates is less effective for this branch.

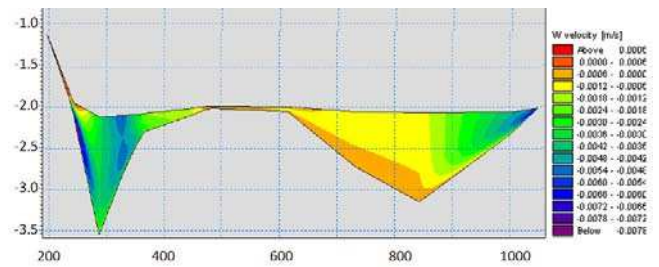


Figure 12. From top to bottom respectively, total velocity, u component, v component and w component of the velocity field on day 11 of simulation.

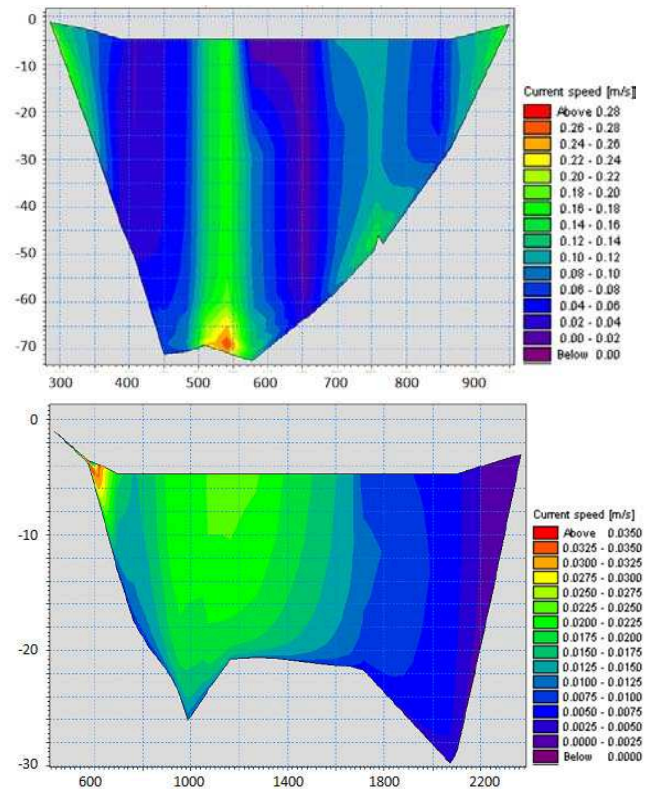
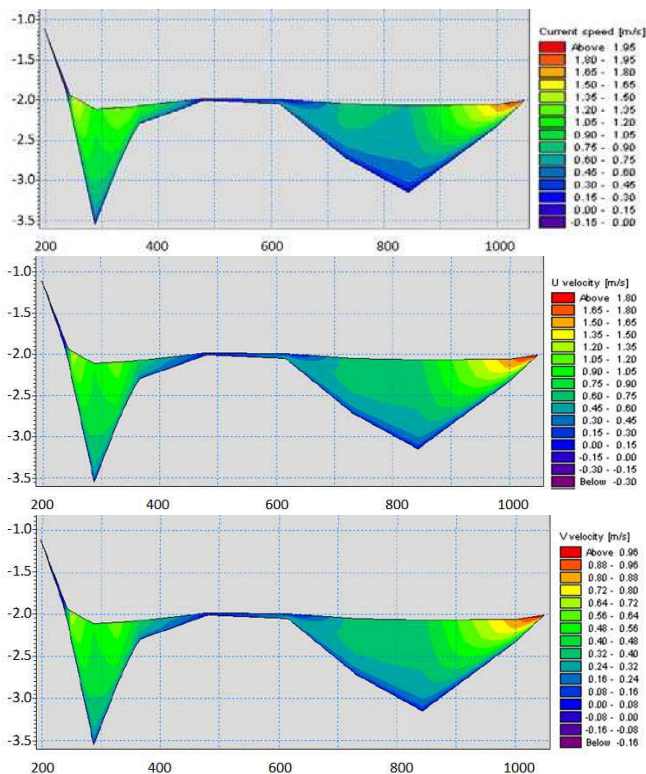


Figure 13. Velocity profile at sections 7 (top) and 9 (bottom) on day 11 of simulation.



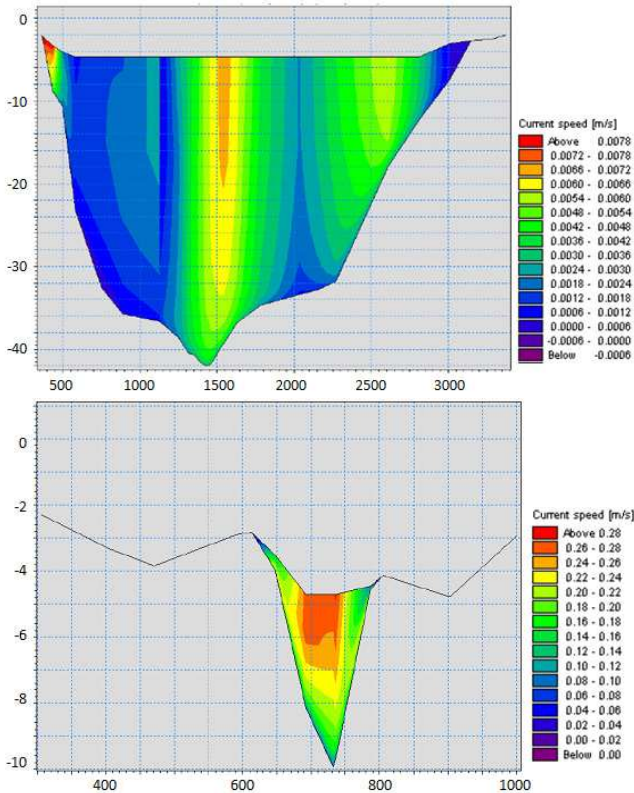


Figure 14. Velocity profile at sections 10 (up) and 12 (down) on day 11 of simulation.

7 CONCLUSION

In this case study, the maximum velocity of the density current is about 2 m/s at the Gazal-Ozan River inflow to the reservoir, but it decreases to about 0.3 m/s when the density current reaches the dam. Maximum velocity is observed at the center of the channel but at some places it is close to the lateral boundaries due to topographic forms. The vertical velocity component is small (less than 0.02 m/s).

The numerical results show good accuracy in simulating the evolution of the density current in the reservoir. Therefore, the model can be reliably used in simulations of flow, sediment transport, and the travel time of the density current in reservoirs, which is needed for the optimal opening and closing of gates for the evacuation of sediments. Another application of such simulations is to determine the operation time of power plants according to the allowed concentration of sediment.

ACKNOWLEDGMENT

The project was supported by the Water Research Institute of Iran. The authors gratefully appreciate the collaboration of the field measurement team.

REFERENCES

- Dan G. Batuca, and Jan M. Jordaan, 2000, " Silting and desilting of reservoirs, "A.A. Balkema/Rotterdam/Brookfield.
- Zhang. H., Xia, M.D., S.J., Li, Z.W., Xia, H.B., Jiang, N.S. & Lin, B.W. 1976. Regulation of sediment in some medium and small sized reservoirs and heavily silt laden streams in China.
- Scheuerlein, H. 1987. Sedimentation of reservoirs-methods of preventing and techniques of rehabilitation. First Iranian Symposium on Dam Engineering, Tehran, Iran.
- Rooseboom, A. 1975a. A sediment-production map for South Africa. Report 61, Department of Water Affairs, Pretoria.
- Rooseboom, A. 1975a. Sedimentneerlating in damkomme. (In Afrikaans). Technical Report 61. Department of Water Affairs, Pretoria, South Africa.
- Sadeghi, M. T. (2003), The evacuation of sediment from the Sefid-Rood Reservoir, MSc thesis, University of Water and Energy Industry, Iran.
- Water Research Institute field measurement group (2007), Field measurement of sediment transport in the Sefid-Rood Reservoir, Technical report.
- Batuca, Dan G. (2000), Silting and Desilting of Reservoirs, A. A. Balkema, Rotterdam, Netherlands.
- Danish Hydraulic Institute (2007), Mike3 Manual, Denmark.
- Tolouie and Esmail (1989), Reservoir Sedimentation and De-siltation, technical report, University of Birmingham, U.K.